Available online at www.sciencedirect.com
SCIENCE DIRECT®
Physics Letters A 324 (2004) 227–234
PHYSICS LETTERS A
www.elsevier.com/locate/pla

Temporal Talbot effect in interference of matter waves from arrays of Bose–Einstein condensates and transition to Fraunhofer diffraction

A. Gammal [a], A.M. Kamchatnov [b,*]

[a] *Instituto de Física, Universidade de São Paulo, C.P. 66318, 05315-970 São Paulo, Brazil*
[b] *Institute of Spectroscopy, Russian Academy of Sciences, Troitsk 142190, Moscow Region, Russia*

Received 18 January 2004; accepted 18 February 2004

Communicated by V.M. Agranovich

Abstract

We consider interference patterns produced by coherent arrays of Bose–Einstein condensates during their one-dimensional expansion. Several characteristic pattern structures are distinguished depending on value of the evolution time. Transformation of Talbot "collapse–revival" behavior to Fraunhofer interference fringes is studied in detail.
© 2004 Elsevier B.V. All rights reserved.

1. Introduction

The interference measurements [1,2] on two expanding Bose–Einstein condensates (BECs) have created new important field of research where the density profile of gas, imaged after releasing from the trap, provides important information about the phase of the ground-state wave function. Expansion of coherent arrays of BECs provides new opportunities to test the phase properties of the system [3–6]. For example, Fraunhofer interference patterns observed in [4] demonstrate strong coherence of BECs confined in separate traps, and experiment [6] shows that this coherence can be manipulated by means of collapses and revivals of wave functions due to nonlinear interaction of BECs in tightly confined states formed by three-dimensional periodic trapping potential.

It is well known (see, e.g., [7]) that mentioned above "collapse–revival" behavior of quantum-mechanical wave functions [8,9] is a temporal counterpart of optical Talbot effect [10,11] in which interference pattern behind the grating restores at distances multiple of the so-called Talbot distance d^2/λ (d is the slit spacing in the grating and λ is the wavelength of light). Similar Talbot effect was also observed in atom optics [12, 13]. Analogy between spatial Talbot effect and temporal collapse–revival behavior of wave functions suggests that such collapses–revivals should exist in interference of matter waves emitted from arrays of BECs provided evolution time is small enough, and indeed such effect was observed in [14]. In this connection it is natural to ask how this short-time Talbot behav-

* Corresponding author.
E-mail address: kamch@isan.troitsk.ru (A.M. Kamchatnov).

0375-9601/$ – see front matter © 2004 Elsevier B.V. All rights reserved.
doi:10.1016/j.physleta.2004.02.064

ior evolves for finite array of condensates to long-time Fraunhofer behavior observed in [4]. This Letter is devoted to consideration of this problem.

In Section 2 we present general formulas for the wave function produced by a linear array of BECs. We confine ourselves with one-dimensional theory under supposition that condensate remains confined in radial direction after turning off a periodic optical potential and evolution takes place only along the axial direction of the BECs array. This formulas permit us to distinguish characteristic stages of evolution—short-time Talbot stage with revivals of the wave function in the central part of the array, intermediate time stage when Fraunhofer fringes already formed with Fresnel diffraction pattern inside each of them, and long-time Fraunhofer stage with standard density distribution along fringes. These stages of evolution of the wave function are studied in detail in Section 3 (Talbot stage) and Section 4 (transition to Fraunhofer stage). The last Section 5 is devoted to conclusions.

2. General formulas

After switching off the periodic optical potential the condensate density decreases and under condition that the initial size $\sim\sigma$ of each BEC is much less than the spacing d between sites, the interatomic interaction can be neglected during most time of the evolution and, hence, the wave function obeys the linear Schrödinger equation

$$i\hbar\psi_t = -\frac{\hbar^2}{2m}\psi_{xx}. \tag{1}$$

If the initial state is given by $\psi(x,0)=\psi_0(x)$, then after time t it evolves into

$$\psi(x,t) = \int_{-\infty}^{\infty} G(x-x',t)\psi_0(x')\,dx', \tag{2}$$

where $G(x-x',t)$ is well-known Green function of Eq. (1) (see, e.g., [15])

$$G(x-x',t) = \sqrt{\frac{m}{2\pi i\hbar t}}\exp\left[\frac{im(x-x')^2}{2\hbar t}\right]. \tag{3}$$

To simplify calculations, we suppose that the initial wave function of BEC in the site of the array with the coordinate kd can be approximated by a Gaussian function and, hence, we represent the initial state of BEC as

$$\psi(x,0) = \frac{1}{\pi^{1/4}\sqrt{\sigma}}\sum_k A_k e^{i\phi_k}\exp\left[-\frac{(x-kd)^2}{2\sigma^2}\right], \tag{4}$$

where $N_k=|A_k|^2$ is equal to number of atoms in kth condensate (we suppose that $\sigma\ll d$) and ϕ_k is its phase. Then Eq. (2) yields the solution

$$\psi(x,t) = \frac{1}{\pi^{1/4}\sqrt{\sigma(1+i\hbar t/m\sigma^2)}} \times\sum_k A_k e^{i\phi_k}\exp\left[-\frac{(x-kd)^2}{2\sigma^2(1+i\hbar t/m\sigma^2)}\right]. \tag{5}$$

This formula should be specified in accordance with the problem under consideration. In the case of large number of condensates in the array confined in axial direction by a parabolic potential, the Thomas–Fermi approximation can be used for calculation of number of atoms in kth condensate which gives [4]

$$N_k = A_k^2 = \frac{15N}{16k_M}\left(1-\frac{k^2}{k_M^2}\right)^2, \tag{6}$$

where

$$k_M = \sqrt{\frac{2\hbar\bar\omega}{m\omega_x^2 d^2}}\left(\frac{15}{8\sqrt{\pi}}N\frac{a}{a_{\rm ho}}\frac{d}{\sigma}\right)^{1/5}, \tag{7}$$

$N=\sum N_k$ is the total number of atoms, $\bar\omega=(\omega_x\omega_\perp^2)^{1/3}$ is the geometric mean of the magnetic trap frequencies, $a_{\rm ho}=\sqrt{\hbar/m\bar\omega}$ is the corresponding oscillator length, and $a>0$ is the s-wave scattering length.

In the experiment [4] there was $k_M\cong 10^2\gg 1$, and this large parameter suggests that there are different stages of evolution.

For

$$t\ll\frac{md^2}{\hbar} \tag{8}$$

each condensate evolves independently of each other and there is no their interference effects.

For

$$t\sim\frac{md^2}{\hbar}\ll k_M\frac{md^2}{\hbar} \tag{9}$$

we have interference between condensates, but in the central part of the array the influence of its finite

size is negligibly small and local interference pattern can be approximated by that of an infinite periodic lattice of condensates which leads to temporal Talbot effect.

For

$$k_M \frac{md^2}{\hbar} \ll t \ll k_M^2 \frac{md^2}{\hbar} \tag{10}$$

the Fraunhofer fringes begin to form. Indeed, their positions are given by (see, e.g., [4])

$$x_n(t) \cong \pm n \frac{2\pi\hbar}{dm} t, \quad n = 0, 1, 2, \ldots, \tag{11}$$

and if t satisfies the condition (10), then distances between neighboring fringes $\sim 2\pi\hbar t/md$ are much greater than the size of each fringe $\sim 2k_M d$ (see below). At the same time, the interference pattern inside each fringe is formed by only some part of the array and hence we get Fresnel diffraction pattern along the fringe.

At last, for

$$t \gg k_M^2 \frac{md^2}{\hbar} \tag{12}$$

we arrive at usual Fraunhofer diffraction when the whole array contributes into interference pattern inside each fringe.

To illustrate these stages of evolution of the wave function, we have shown in Fig. 1 the distributions of density $\rho = |\psi|^2$ calculated from formulas (5)–(7) with $\phi_k = 0$ (coherent condensates). We see that for $t \ll k_M(md^2/\hbar)$ the density distribution reproduces periodically in time with period $t_r \sim md^2/\hbar$ (see exact formula (20)), the side fringes begin to form at $t \sim k_M(md^2/\hbar)$, and for $t \gg k_M(md^2/\hbar)$ there are peaks of density at the coordinates given by (11) and profiles of fringes take Fraunhofer form for $t \gg (k_M d)^2 m/\hbar$. The solution (5) permits us to investigate these stages of evolution analytically.

3. Talbot revivals of wave function

For time values in the region (9), we can approximate the array by infinite lattice of equidistant condensates so that for coherent condensates their wave function is given by

$$\psi(x,t) = \frac{A}{\pi^{1/4}\sqrt{\sigma(1 + i\hbar t/m\sigma^2)}} \times \sum_{k=-\infty}^{\infty} \exp\left[-\frac{(x - kd)^2}{2\sigma^2(1 + i\hbar t/m\sigma^2)}\right]. \tag{13}$$

With the use of definition of θ_3-function (see, e.g., [16])

$$\theta_3(z,\tau) = \sum_{k=-\infty}^{\infty} \exp\left[i\pi\left(\tau k^2 + 2zk\right)\right] \tag{14}$$

the wave function (13) can be presented in the form

$$\psi(x,t) = \frac{\pi^{1/4} A}{d}\sqrt{\frac{2\sigma i}{\tau}} \exp\left(-\frac{i\pi x^2}{d^2\tau}\right)\theta_3\left(\frac{x}{d\tau}, -\frac{1}{\tau}\right), \tag{15}$$

where

$$\tau = \frac{2\pi i\sigma^2}{d^2}\left(1 + \frac{i\hbar t}{m\sigma^2}\right). \tag{16}$$

By means of transformation formula (see [16])

$$\theta_3\left(\frac{z}{\tau}, -\frac{1}{\tau}\right) = \sqrt{-i\tau}\exp\left(\frac{i\pi z^2}{\tau}\right)\theta_3(z,\tau) \tag{17}$$

we transform (15) into

$$\psi(x,t) = \frac{\sqrt{2\pi\sigma}A}{\pi^{1/4}d}\theta_3\left(\frac{x}{d}, \tau\right). \tag{18}$$

Then the periodicity property of θ_3-function, $\theta_3(z, \tau \pm 2) = \theta_3(z,\tau)$, leads at once to the periodicity of the wave function,

$$\psi(x, t + t_r) = \psi(x,t), \tag{19}$$

with the period

$$t_r = \frac{md^2}{\pi\hbar}. \tag{20}$$

If the array of BECs is realized in optical periodic potential with light wavelength λ, then the spacing between neighboring lattice sites is equal to $d = \lambda/2$ and the revival time can be expressed in the form

$$t_r = \frac{1}{4}\frac{2\pi\hbar}{E_R}, \tag{21}$$

where

$$E_R = \frac{\hbar^2 q^2}{2m} \tag{22}$$

is the recoil energy ($q = 2\pi/\lambda$).

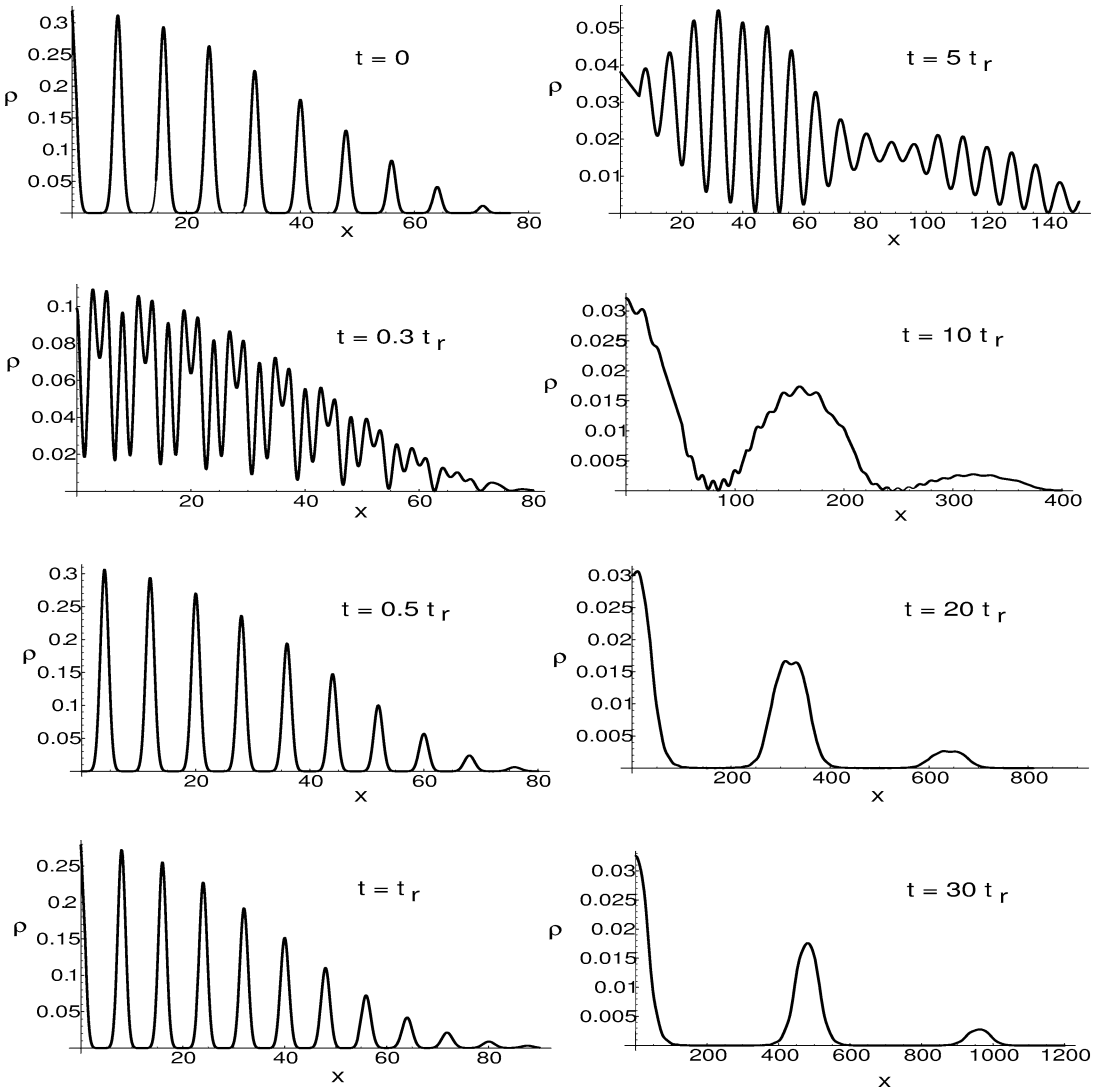

Fig. 1. Evolution of the density profile of array of condensates with time calculated according to Eqs. (5)–(7) with $d = 8$, $\sigma = 1$ (in dimensionless units) and $k_M = 10$. At $t = 0.3t_r$, where t_r is given by Eq. (20), we see complex interference pattern ("collapse" of wave function); at $t = 0.5t_r$ the central part coincides with that for $t = 0$ but shifted to a half-period $d/2$; at $t = t_r$ the initial distribution is almost completely restored; at $t = 5t_r$ the side fringes start to form, and, finally, at $t = 30t_r$ we see Fraunhofer diffraction of matter waves from finite "grating".

The evolution time $t_r/2$ corresponds to the transformation of θ_3-function $\theta_3(z, \tau + 1) = \theta_4(z, \tau) = \theta_3(z + 1/2, \tau)$, that is we obtain the wave function shifted to the distance $d/2$ with respect to its initial form:

$$\psi(x, t + t_r/2) = \psi(x + d/2, t). \tag{23}$$

Above calculation explains periodic restoration of initial wave function by means of transformation properties of θ-functions. To relate this approach with standard one (see, e.g., [9]), let us consider the problem from a different point of view. The linear Schrödinger equation (1) with periodic initial condition

$$\psi(x, 0) = \frac{A}{\pi^{1/4}\sqrt{\sigma}} \sum_{k=-\infty}^{\infty} \exp\left[-\frac{(x - kd)^2}{2\sigma^2}\right] \tag{24}$$

can be solved by the Fourier method which gives

$$\psi(x,t) = \frac{\sqrt{2}\pi^{1/4}A}{d} \times \left\{1 + 2\sum_{k=1}^{\infty} \exp\left[-\frac{2\pi^2\sigma^2}{d^2}\left(1 + \frac{i\hbar t}{m\sigma^2}\right)k^2\right] \times \cos\left(\frac{2\pi x}{d}k\right)\right\}. \quad (25)$$

(The relationships between presentations (13) and (25) of the same wave function $\psi(x,t)$ is expressed by the known identity for these two series; see, e.g., [17].) We see that at t equal to multiple of Talbot time t_r, $t = nt_r$, all phase factors in (25) become equal to unity and (25) reduces to the Fourier series for the initial periodic wave function (24). This method of derivation of time-periodicity of the wave function shows that periodic restoration of the initial state is not a specific feature of the initial state (24) built of Gaussian functions. Indeed, any periodic initial function can be expanded into Fourier series and harmonics $\cos(2\pi xk/d)$, $k = 1, 2, \ldots$, evolve with time according to factors $\exp(-i\frac{2\pi^2\hbar t}{md^2}k^2)$ which become equal to unity at $t = nt_r$. Thus, any periodic initial wave function completely restores periodically its form. The described above picture of periodic in time changes of the interference pattern is shown in Fig. 2 where even for relatively small number of condensates first several revivals are clearly seen.

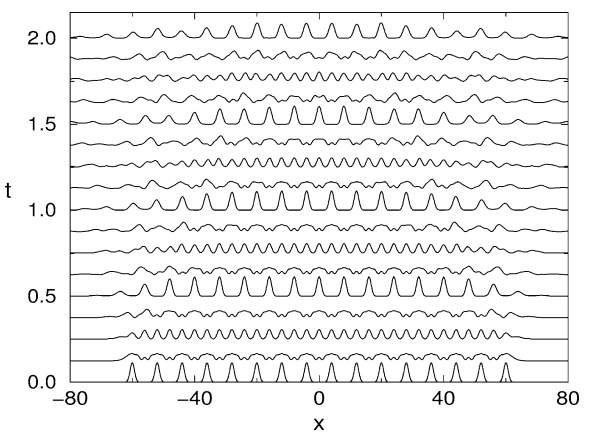

Fig. 2. Evolution of density profiles for BEC arrays with zero relative phase. Two first revivals at $t = nt_r$, $n = 1, 2$, are clearly seen as well as "fractional revivals" at intermediate moments $t_r/8$, $t_r/4$, $3t_r/8$, $t_r/2$, etc.

The above theory can be generalized on non-zero phases in the initial state and hence in the solution (2). For example, in the case of alternating phases of condensates,

$$e^{i\phi_k} = (-1)^k, \quad (26)$$

the wave function can be expressed in terms of θ_4-function [16],

$$\psi(x,t) = \frac{\pi^{1/4}A}{d}\sqrt{\frac{2\sigma i}{\tau}} \times \exp\left(-\frac{i\pi x^2}{d^2\tau}\right)\theta_4\left(\frac{x}{d\tau}, -\frac{1}{\tau}\right), \quad (27)$$

or, with the use of the transformation formula [16],

$$\theta_4\left(\frac{z}{\tau}, -\frac{1}{\tau}\right) = \sqrt{-i\tau}\exp\left(\frac{i\pi z^2}{\tau}\right)\theta_2(z,\tau), \quad (28)$$

in the form

$$\psi(x,t) = \frac{\sqrt{2\pi\sigma}A}{\pi^{1/4}d}\theta_2\left(\frac{x}{d}, \tau\right). \quad (29)$$

Then the property $\theta_2(z, \tau + 1) = \exp(\pi i/4)\theta_2(z,\tau)$ leads to restoration of the initial state (up to inessential constant phase factor) after revival time

$$t_r = \frac{md^2}{2\pi\hbar} = \frac{1}{8}\frac{2\pi\hbar}{E_R}. \quad (30)$$

Let us estimate an order of magnitude of the revival time for arrays of BECs. In the case [6] of ^{87}Rb BECs array loaded into optical potential with light wavelength $\lambda = 838$ nm formula (21) gives $t_r \simeq 75$ μs. This is about one order of magnitude less than the revival time, caused by nonlinear interaction, of single condensate in the experiment [6]. In this experiment absorption images were taken after a time-of-flight period of 16 ms which is much greater (with factor ~ 200) than our estimate of t_r. For number of sites in 3D lattice $\sim 10^3$ we have $k_M \sim 10$ and, hence, the observed interference patterns correspond to the Fraunhofer limit (12). In this case the difference of interference patterns was caused by difference in initial states of condensates at different "hold times" of evolution of each condensate in strongly confined states formed by 3D periodic trapping potential.

In the experiment [4] the revival time is $t_r \simeq 69$ μs and a typical image was taken at $t = 29$ ms, that is for $k_M \sim 100$ again in the Fraunhofer limit (in accordance with the theory developed in this Letter).

4. Transition to Fraunhofer interference

Now we shall turn to the regions (10) and (12). Effects of Fresnel diffraction can be noticed in Fig. 1 for $t = 10t_r$. However, they are not expressed clearly enough because of smooth distribution (6) of density in the array used in our calculations. Therefore it is more instructive to consider finite array with equal amplitudes $A_k = 1$ of wave functions in each condensate and take $\phi_k = \Delta\phi \cdot k$, that is with equal differences $\Delta\phi$ of phases between neighboring condensates. Then Eq. (5) with $t \gg m\sigma^2/\hbar$ reduces to

$$\psi(x,t) \cong \frac{1}{\pi^{1/4}}\sqrt{\frac{m\sigma}{i\hbar t}}e^{\frac{imx^2}{2\hbar t}}e^{-\frac{m\sigma^2x^2}{2\hbar^2t^2}} \times \sum_{k=-k_M}^{k_M}\exp\left[-i\left(\frac{mdx}{\hbar t}-\Delta\phi\right)k+\frac{imd^2}{2\hbar t}k^2\right], \tag{31}$$

where we have taken into account only leading real and imaginary contributions in the series expansion of the exponential in powers of $m\sigma^2/\hbar t$. The sum here has maximal amplitude when all terms are in phase in linear in k approximation. This condition defines coordinates x_n of the centers of fringes,

$$x_n = \frac{2\pi\hbar}{md}\left(n+\frac{\Delta\phi}{2\pi}\right)t, \quad n = 0, \pm1, \pm2, \ldots. \tag{32}$$

To consider profiles of fringes, we introduce the coordinate δ which is reckoned from the center of the fringe:

$$x = x_n + \delta, \tag{33}$$

so that dependence on δ is determined mainly by the factor

$$\Phi(\delta,t) = \sum_{k=-k_M}^{k_M}\exp\left(-\frac{imd\delta}{\hbar t}k+\frac{imd^2}{2\hbar t}k^2\right). \tag{34}$$

If t satisfies the condition (10), then both terms in the exponential have the same order of magnitude and, on one hand, the fringe width is of order of magnitude of the array length, $\delta \sim 2k_Md$, and, on the other hand, it is much less than the distance between fringes. Therefore the coordinate x in the factor $\exp(-m^2\sigma^2x^2/2\hbar^2t^2)$ can be replaced by x_n. Thus, the wave function in vicinity of the nth fringe is given by

$$\psi_n(x,t) = \frac{1}{\pi^{1/4}}\sqrt{\frac{m\sigma}{i\hbar t}}e^{\frac{imx^2}{2\hbar t}} \times \exp\left[-\frac{2\pi^2\sigma^2}{d^2}\left(n+\frac{\Delta\phi}{2\pi}\right)^2\right]\Phi(\delta,t), \tag{35}$$

where $\delta = x - x_n$. Now, for $k_M \gg 1$ the sum in (34) can be approximated by integrals which are easily

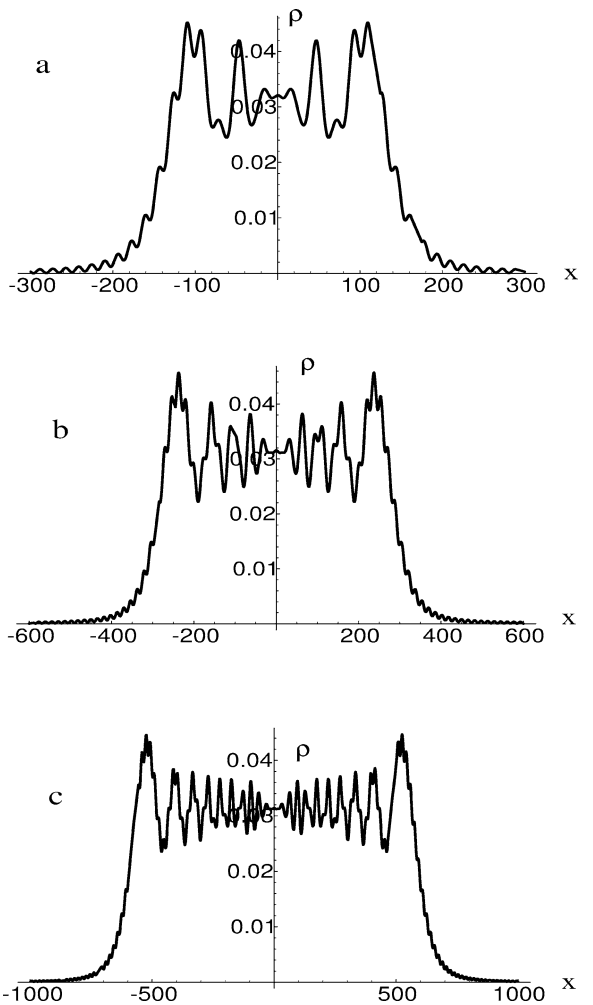

Fig. 3. The central fringe profile for several values of the number of sites in the array. Time t corresponds to the region (10). The plots are calculated for $d = 8$, $\sigma = 1$ and (a) $k_M = 20$ at $t = 40t_r$; (b) $k_M = 40$ at $t = 80t_r$; (c) $k_M = 80$ at $t = 160t_r$. Formation of the Fresnel pattern is clearly seen.

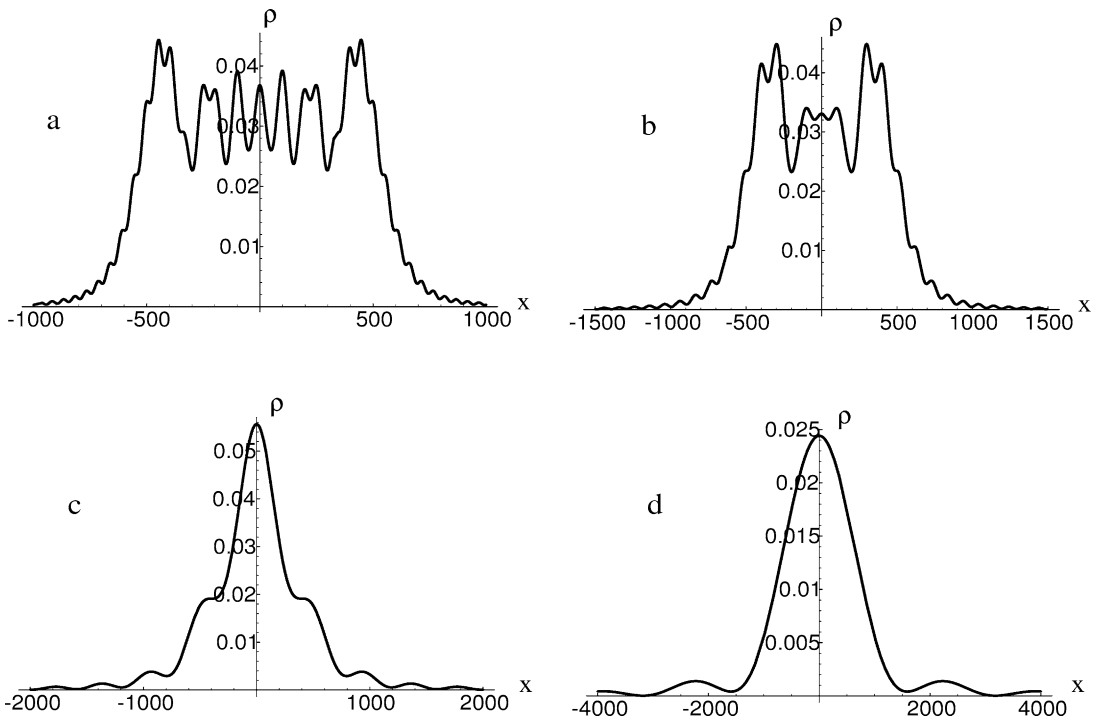

Fig. 4. Evolution of density profile of central fringe on time. Values of the parameters are equal to $d = 8$, $\sigma = 1$, $k_M = 80$ and (a) $t = 500t_r$; (b) $t = 1000t_r$; (c) $t = 2000t_r$; (d) $t = 16000t_r$. Transformation of Fresnel profile shown in Fig. 3(c) to standard Fraunhofer profile is clearly seen.

expressed in terms of Fresnel functions [18]:

$$\Phi(\delta,t) = \sqrt{\frac{\pi\hbar t}{md^2}}\, e^{\frac{im\delta^2}{2\hbar t}} \times \left[\mathrm{C}\left(\sqrt{\frac{m}{2\hbar t}}(k_M d+\delta)\right) + \mathrm{C}\left(\sqrt{\frac{m}{2\hbar t}}(k_M d-\delta)\right) + i\left(\mathrm{S}\left(\sqrt{\frac{m}{2\hbar t}}(k_M d+\delta)\right) + \mathrm{S}\left(\sqrt{\frac{m}{2\hbar t}}(k_M d-\delta)\right)\right)\right]. \quad (36)$$

Thus, distribution of density in the nth fringe is given by

$$|\psi_n|^2 = \frac{\sqrt{\pi}\sigma}{d^2}\exp\left[-\frac{4\pi^2\sigma^2}{d^2}\left(n+\frac{\Delta\phi}{2\pi}\right)^2\right] \times \left\{\left[\mathrm{C}\left(\sqrt{\frac{m}{2\hbar t}}(k_M d+\delta)\right) + \mathrm{C}\left(\sqrt{\frac{m}{2\hbar t}}(k_M d-\delta)\right)\right]^2 + \left[\mathrm{S}\left(\sqrt{\frac{m}{2\hbar t}}(k_M d+\delta)\right) + \mathrm{S}\left(\sqrt{\frac{m}{2\hbar t}}(k_M d-\delta)\right)\right]^2\right\}. \quad (37)$$

The exponential factor determines the number of atoms in the nth fringe:

$$N_n = \text{const} \times \exp\left[-\frac{4\pi^2\sigma^2}{d^2}\left(n+\frac{\Delta\phi}{2\pi}\right)^2\right]. \quad (38)$$

This formula reduces to Eq. (6) of Ref. [4] for $\Delta\phi = 0$. Dependence on δ determines fine interference pattern inside fringes. It is expressed by the factor in curly brackets and demonstrates typical Fresnel form (see, e.g., [15, Section 3.3], or [19, Section 8.7]) of diffraction from a slit with width $2k_M d$ equal to the whole array length. Accuracy of this analytical description

depends on the number of sites in the array and increases with growth of k_M. In Fig. 3 it is shown how exact profile of density along the fringe changes with increase of k_M. Its transformation into Fresnel diffraction pattern is clearly seen. Small "ripples" are obviously caused by the discrete structure of the array.

For larger values of time (12) Fresnel structure evolves into usual form of density distribution in Fraunhofer diffraction from finite slit with width $2k_M d$. In this limit of very large t the quadratic in k tern in exponentials in Eq. (34) is much less than unity and can be omitted. Then simple integration gives $\Phi(\delta, t) = \frac{2\hbar t}{nd\delta} \sin(\frac{mk_M d\delta}{\hbar t})$ and hence distribution of density inside fringes is proportional to

$$\left|\Phi(\delta, t)\right|^2 = 4\frac{\sin^2(mk_M d\delta/\hbar t)}{(md\delta/\hbar t)^2} \tag{39}$$

which is standard Fraunhofer diffraction distribution from finite slit (see, e.g., [19, Section 8.5]). The described here evolution of profile is illustrated in Fig. 4. The total intensity of nth fringe is still determined, of course, by Eq. (38).

5. Conclusion

We have presented in this Letter analysis of interference of matter waves during one-dimensional expansion of finite arrays of condensates. It shows that the interference pattern exhibits quite complicated evolution with time from Talbot "collapses and revivals" of wave function through intermediate region of Fraunhofer fringes with Fresnel patterns inside them, and, eventually, to standard Fraunhofer diffraction from finite grating. One may suppose that technique of density imaging will permit one to study experimentally all these stages.

Acknowledgements

This work was supported by FAPESP (Brazil) and CNPq (Brazil). A.M.K. thanks also RFBR for partial support.

References

[1] M.R. Andrews, C.G. Townsend, H.-J. Miesner, D.S. Durfee, D.M. Kurn, W. Ketterle, Science 275 (1997) 637.
[2] Y. Shin, M. Saba, T.A. Paquini, W. Ketterle, D.E. Pritchard, A.E. Leanhardt, cond-mat/0306305.
[3] C. Orzel, A.K. Tuchman, M.L. Fenselau, M. Yasuda, M.A. Kasevich, Science 291 (2001) 2386.
[4] P. Pedri, L. Pitaevskii, S. Stringari, C. Fort, S. Burger, F.S. Cataliotti, P. Maddaloni, F. Minardi, M. Inguscio, Phys. Rev. Lett. 87 (2001) 220401.
[5] M. Greiner, I. Bloch, O. Mandel, Th.W. Hänsch, T. Esslinger, Phys. Rev. Lett. 87 (2001) 160405.
[6] M. Greiner, O. Mandel, Th.W. Hänsch, I. Bloch, Nature 419 (2002) 51.
[7] M. Berry, I. Marzoli, W. Schleich, Phys. World 14 (6) (2001) 39.
[8] J.H. Eberly, N.B. Narozhny, J.J. Sanchez-Mondragon, Phys. Rev. Lett. 44 (1980) 1323.
[9] I.Sh. Averbukh, N.F. Perelman, Usp. Fiz. Nauk 161 (1991) 41, Sov. Phys. Usp. 34 (1991) 572.
[10] H.F. Talbot, Philos. Mag. 9 (1836) 401.
[11] K. Patorski, Prog. Opt. 28 (1989) 1.
[12] J.F. Clauser, S. Li, Phys. Rev. A 49 (1994) R2213.
[13] M.S. Chapman, C.R. Ekstrom, T.D. Hammond, J. Schmiedmayer, B.E. Tannian, S. Wehinger, D.E. Pritchard, Phys. Rev. A 51 (1995) R14.
[14] L. Deng, E.W. Hagley, J. Denschlag, J.E. Simsarian, M. Edwards, C.W. Clark, K. Helmerson, S.L. Rolston, W.D. Phillips, Phys. Rev. Lett. 83 (1999) 5407.
[15] R.P. Feynman, A.R. Hibbs, Quantum Mechanics and Path Integrals, McGraw–Hill, New York, 1965.
[16] H. Bateman, A. Erdélyi, Higher Transcendental Functions, vol. 2, McGraw–Hill, New York, 1953.
[17] D. Mumford, Tata Lectures on Theta I, Birkhäuser, Boston, 1983.
[18] I.S. Gradshteyn, I.P. Ryzhik, Tables of Integrals, Series, and Products, Academic Press, New York, 1965.
[19] M. Born, E. Wolf, Principles of Optics, Pergamon, Oxford, 1968.